Biotechnology and Bioprocess Engineering 20: 825-833 (2015)
DOI 10.1007/s12257-015-0233-7

RESEARCH PAPER

Efficient CRISPR/Cas9-mediated Multiplex Genome Editing in CHO Cells *via* High-level sgRNA-Cas9 Complex

Jongoh Shin, Namil Lee, Yoseb Song, Jinhyung Park, Taek Jin Kang, Sun Chang Kim, Gyun Min Lee, and Byung-Kwan Cho

Received: 3 April 2015 / Revised: 27 May 2015 / Accepted: 7 June 2015
© The Korean Society for Biotechnology and Bioengineering and Springer 2015

Abstract Increasing demand for recombinant therapeutic proteins has warranted the need for an efficient host cell to produce high-quality proteins, with a high yield. Chinese hamster ovary (CHO) cells appear to meet this demand, and their genetic tailoring will facilitate improvements in their productivity for recombinant proteins. Recent advances in programmable RNA-guided Cas9 nuclease (RGN) have facilitated CHO cell engineering *via* site-specific genome editing. One critical determinant for increasing genome-editing efficiency is attaining a balanced expression level of Cas9 nuclease and guide RNAs in the nucleus. Here, we achieved high-level expression of Cas9 nuclease and single guide RNA (sgRNA), enhancing expression levels approximately three-fold over the conventional methodology by using an iterative transfection approach. We demonstrated that high abundance of sgRNA and Cas9 nuclease induced a two-fold increase in the site-specific mutation rate on average for both single and multiple genetic targets. Sequencing results confirmed frame-shift mutations at targeted genomic loci created by error-prone NHEJ-associated mutations. Moreover, we controlled the amount of sgRNA-Cas9 complex formation *in vitro* and delivered the complex directly to cells, resulting in the maximization of mutation frequency by the high-level of sgRNA-Cas9 complex. Importantly, mutation rates of putative off-target sites remained minimal in spite of the improved genome-editing efficiency. These results provide an efficient strategy for editing the CHO genome with the reduction of the time-consuming screening efforts aimed at isolating clones with desirable properties.

Keywords: genome editing, CRISPR/Cas9, Chinese hamster ovary (CHO) cells,iterative transfection

Jongoh Shin†, Namil Lee†, Yoseb Song, Jinhyung Park, Sun Chang Kim, Gyun Min Lee, Byung-Kwan Cho
Department of Biological Sciences, Korea Advanced Institute of Science and Technology, Daejeon 305-701, Korea

Jongoh Shin, Namil Lee, Yoseb Song, Sun Chang Kim, Byung-Kwan Cho
KI for the BioCentury, Korea Advanced Institute of Science and Technology, Daejeon 305-701, Korea

Taek Jin Kang
Department of Chemical and Biochemical Engineering, Dongguk University-Seoul, Seoul 100-715, Korea

Sun Chang Kim, Byung-Kwan Cho*
Intelligent Synthetic Biology Center, Daejeon 305-701, Korea
Tel: +82-42-350-2660; Fax: +82-42-350-5620
E-mail: bcho@kaist.ac.kr

†These authors equally contributed to this work.

1. Introduction

CHO cells are the most widely used mammalian hosts for the industrial production of recombinant therapeutic proteins, which range widely from cytokines to monoclonal antibodies [1]. The allure of recombinant protein expression in CHO cell lines stems from their capacity to implement human-like post-translational modifications. In an effort to increase their volumetric productivity and quality, CHO cells are often the subjects of reengineering efforts, with a particular focus on improving the glycosylation homogeneity for target proteins [2,3].

With the recent availability of genome sequences and genome-editing technologies, it has become possible to create CHO cells with more desirable characteristics through the use of nuclease-based site-specific manipulation of genomic sequences [4-7]. In particular, zinc finger nucleases (ZFNs) and transcription activator-like effector nucleases

(TALENs) have been used as target-specific genome editing tools to induce DNA double-strand breaks (DSBs) that stimulate error-prone non-homologous end joining (NHEJ) or homology-directed repair (HR) for target gene disruption [8]. Furthermore, the efficient site-specific mutagenesis will reduce the need for time-consuming screening efforts, whereby large populations of clones are screened for desirable genetic properties. In spite of their advantages, ZFN and TALEN are limited by the requirement that each target-specific nuclease be specifically designed for their given target sequence, a requisite which becomes challenging in the context of large-scale multiplex genome editing interests. In contrast, programmable RGN, derived from the type II prokaryotic clustered regularly interspaced short palindromic repeats (CRISPR) adaptive immune system, is an efficient target-specific genome editing tool that enables single or multiple site-directed mutagenesis in many species [9-15]. RGN-mediated genome editing has been used to generate genetically tractable transgenic models, identify phenotypically important genes at the genome-level scale, modulate transcriptional regulation, and control epigenetic states [16]. However, in order for the insertion/deletion (indel) rate of CRISPR to be improved, several factors need to be addressed, one of which is the regulation of guide RNA and Cas9 nuclease expression levels in the nucleus. To this end, it has previously been demonstrated that high-level expression of Cas9 nuclease or treatment with cell-penetrating peptide-tagged Cas9 nuclease increases the indel rate in mammalian cells [16-18].

Since CHO cell populations show genetic instability and clonal variation, a highly efficient genome editing method is needed in order to reduce the burden of subsequent screening or isolation efforts associated with procuring CHO cells with engineered characteristics [19,20]. Here, we control the high-level expression of Cas9 nuclease and sgRNA for multiplex CHO genome editing by using an iterative transfection protocol. After several rounds of repetitive transfection, an approximate three-fold enhancement in Cas9 nuclease and sgRNA expression was achieved over the conventional, single transfection approach. We further demonstrated that the abundance of Cas9 nuclease and sgRNA induced a two-fold increase in the site-specific mutation rate, on an average, for both single and multiple genetic targets while maintaining a low rate of off-target effects.

2. Materials and Methods

2.1. Cell culture and repetitive transfection

CHO cells were grown in Dulbecco's modified Eagle's medium (DMEM; Gibco, Grand Island, NY, USA) supplemented 10% fetal bovine serum (Gibco) and 0.5 mg/mL Geneticin (GEBCO BRL, Grand Island, NY, USA) at 37°C in a humidified incubator (Panasonic, Wood Dale, IL, USA) with 5% CO_2. For transfection, CHO cells at a density of 5×10^5 cells per well were grown overnight in 6-well plates containing DMEM supplemented with 10% fetal bovine serum. The following day, the cells were transfected with 2.5 μg of RGN plasmid or sgRNA-Cas9 nuclease complex and 8 μL of Lipofectamine® 2000 (Invitrogen, Grand Island, NY, USA), followed by incubation at 37°C for 8 h. For sgRNA-Cas9 nuclease complex delivery *in vitro*, Cas9 protein (100 nM) was mixed with *in vitro* transcribed sgRNA (0.1 ~ 150 nM) dissolved in nuclease-free water and incubated for 10 min at room temperature before use.

2.2. Plasmid construction

The plasmid (pX330) encoding the Cas9 nuclease was obtained from Addgene (plasmid 42230). Oligonucleotides for the sgRNA (Table 1) were annealed and inserted into the pX330 *Bbs*I cloning site. The pEGFP-C1 plasmid (Clontech, Oxford, UK) was used to establish CHO-K1 cells stably expressing a chromosomally integrated GFP. The primers (Forward: 5′-GGGAGCGGCCGCGAGGGC CTATTTCCCATGAT and Reverse: 5′-CGCCCCTGC AGGCGGGCCATTTACCGTAAGTTAT) were used to construct the pX330d_E_T plasmid. Briefly, from the pX330-Thbs1 vector, an amplicon (sgRNA expression cassette) was generated by PCR using primers containing two restriction sites. Subsequently, pX330-Efemp1 and the

Table 1. Oligonucleotides used in the construction of sgRNA

Direction	Gene	Sequence (5′ to 3′)
Sense	*GFP*	CACCGAAGTTCGAGGGCGACACCC
	Efemp1	CACCGCAACCAGTGGTGTGGTGCC
	Fos	CACCGGAGGATGACGCCTCGTAGT
	Thbs1	CACCGTCCGGCCGACGACTGGTAAA
Antisense	*GFP*	AAACGGGTGTCGCCCTCGAACTTC
	Efemp1	AAACGGCACCACACCACTGGTTGC
	Fos	AAACACTACGAGGCGTCATCCTCC
	Thbs1	AAACTTTACCAGTCGTCGGCCGGAC

PCR amplicon were digested by NotI and Sbf1 and further purified on a 2% agarose TBE gel by using the QIAEX II Gel Extraction Kit (Qiagen, Crawley, UK). Digested fragments were mixed with Quick Ligase (NEB, Ipswich, MA) and T4 DNA Ligase buffer (NEB, Ipswich, MA), followed by incubation at 37°C for 10 min in order to obtain the pX330d_E_T vector.

2.3. Flow cytometry

Two days post-transfection, cells were harvested and resuspended in DMEM supplemented with 10% fetal bovine serum. The cells were filtered through a 40 μm cell strainer (BD Biosciences, San Jose, CA, USA) to obtain a single-cell suspension. FACS analysis was performed on a FACSAria II (BD bioscience), using a 488 nm laser and an FITC channel 530/30 filter for GFP experiments. Quantitation was carried out using FlowJo software (Tree Star, Ashland, OR, USA).

2.4. T7E1 assay and TA-cloning based sequencing

At 48 h post-transfection, genomic DNA was extracted using the Wizard genomic DNA purification kit (Promega, Madison, WI, USA). PCR was then performed to generate PCR amplicons containing RGN target sites (Table 2). PCR amplicons were denatured and annealed to form heteroduplexes. PCR products were digested with T7 endonuclease 1 (NEB, Ipswich, MA, USA) for 20 min at 37°C, and subsequently analyzed by 2% agarose gel electrophoresis. For sequencing analysis, the purified amplicons were cloned into the pGEM®-T Easy vector (Promega), and the cloned products were sequenced using the 3730xl DNA Analyzer (Applied Biosystems, Grand Island, NY, USA).

2.5. qRT-PCR analysis

Total RNA was extracted with TRIzol reagent (Invitrogen), and 1 μg of total RNA was reverse-transcribed with random hexamers by using the SuperScript III First-Strand Synthesis System (Invitrogen). qPCR analysis was performed with custom primers (Forward: 5′- GGTGTGGTGCCGTTT TAGAG and Reverse: 5′-CGGTGCCACTTTTTCAAGTT), using iQ SYBR Green Supermix (Bio-Rad, Hercules, CA, USA) on a CFX96 Real-time system. The relative intensity of mRNA was normalized to the relative intensity measured for β-actin, which was used as an endogenous control.

2.6. Western-blot analysis

CHO cells were harvested and lysed in RIPA buffer (50 mM Tris-HCl (pH 7.4), 150 mM NaCl, 1% NP40, 0.1% SDS, 0.25% sodium deoxycholate, 1 mM EDTA,

Table 2. Oligonucleotides used in the confirmation of genome editing

1st PCR			
		Forward (5′ to 3′)	Reverse (5′ to 3′)
On-target	*GFP*	ATGCGGTTTTGGCAGTACAT	TTGTACAGCTCGTCCATGCC
	Efemp1	TCCATCTCGTGTGTTGCTCT	TGCTTGGGCTTAAAAACCAG
	Fos	CCCCCAAAGACCCTTATTGT	AGCATCACTCGCTTGAAAGG
	Thbs1	CACCTTGCTTTTGTCCTGGT	CTCAGCGCTCTCCATCTTCT
Off-target	GFP-Off1	GGCAGCTGTATGTAAACTCTCCA	TCCTCAGTCTGCTCCAACCT
	Efemp1-Off1	CTGAGGCTGGCTTTGAACTC	CCATCTCTGCTCTGGGAAGT
	Efemp1-Off2	GGGAAACTGACTTGACTTCATTG	GGGATCCAACTGAGGCCTAT
	Efemp1-Off3	ACCAGAGTGCTGGGATTGAG	CTGAAGGGAAAGGGAGGAAC
	Efemp1-Off4	CTTTTCTCCCCGTGTCTCTG	ATCAGCCTTGTTGACCTGCT
	Efemp1-Off5	GCAATAGTTCATTTTCCAGCA	TCCTAATAGTCCCATGAGGTAGG
	Thbs1-Off1	ACATTCCCAGGGACTCACAC	TTTGTATTCCACCCCATGCT
2nd PCR			
		Forward (5′ to 3′)	Reverse (5′ to 3′)
On-target	*GFP*	CCTGAAGTTCATCTGCACCA	GAACTCCAGCAGGACCATGT
	Efemp1	GGAGGATACCTCTGCCTTCC	CTTGGCCACTGAGAAGCATT
	Fos	GGAGGATACCTCTGCCTTCC	CCCAGGCTCTAGTTAGCGAGT
	Thbs1	GGGGGTACAAGATAGCTCAGG	CGTTGGAGACCACACTGAAG
Off-target	GFP-Off1	GACCTCAATCTCTGCCCTCA	GTAGGAGGATAAATGGCCAAA
	Efemp1-Off1	CCACAGCTCATTGGCTTTTT	GTGCCCTACGTGTCCAGTTT
	Efemp1-Off2	AGGCAAGGGTCAGAAGAGGT	GGGGACAGGCATTGTATTTG
	Efemp1-Off3	TTGATTTGGGAAATGATCCA	GCGCTGCTCACTGTAAATCA
	Efemp1-Off4	ACCTAGCACCCAGCACCTC	AGATGCTCTGGACGATCTTG
	Efemp1-Off5	CATCCACAACCCAAACAGC	GTTGGCACTCTGCACTGGTA
	Thbs1-Off1	CCGATTACCCCAAATCATTG	AAATCCATGCTGGAACCAAG

and a phosphatase inhibitor cocktail). Samples containing 5 μg of total protein were separated on 10% SDS-polyacrylamide gels and electrophoretically transferred to PVDF membranes. After blocking with 5% skimmed milk, the membranes were incubated with primary antibodies against the FLAG epitope at 1:30,000 dilution (Sigma, USA) or β-actin at 1:10,000 (Abcam, Cambridge, MA, USA) and with an HRP-labeled secondary antibody (ThermoFisher Scientific, Waltham, MA, USA) for 1 h at room temperature.

2.7. Purification of Cas9 protein

E. coli BL21 (DE3) strain was transformed with the plasmid pET28a/Cas9-Cys containing Cas9 protein fused to an N-terminal 6x His-tag [17]. Cas9 protein was purified using Ni-NTA agarose resin (Qiagen, CA, USA), and dialyzed against 50 mM Tris-HCl (pH 8.0), 200 mM KCl, 0.1 mM EDTA, 1 mM DTT, 0.5 mM PMSF and 20% glycerol.

2.8. sgRNA preparation

RNA was *in vitro* transcribed through run-off reactions by T7 RNA polymerase using the MEGAshortscript T7 kit (Ambion, CA, USA). pX330-Fos plasmid serves as the PCR template to generate a template DNA with custom primers (Forward: 5′- GGAAAAAATTAATACGACTCACTATAG GGGGAGGATGAC GCCTCGTAGT and Reverse: 5′- AAA AAAGCACCGACTCGGTGCCA) for sgRNA transcription. *In vitro* transcribed RNA was purified in denaturing PAGE, phenol-chloroform-extracted and ethanol precipitation.

3. Results and Discussion

3.1. RGN-mediated genome editing by using iterative transfection

RGN-mediated DNA DSBs at specific genomic loci are

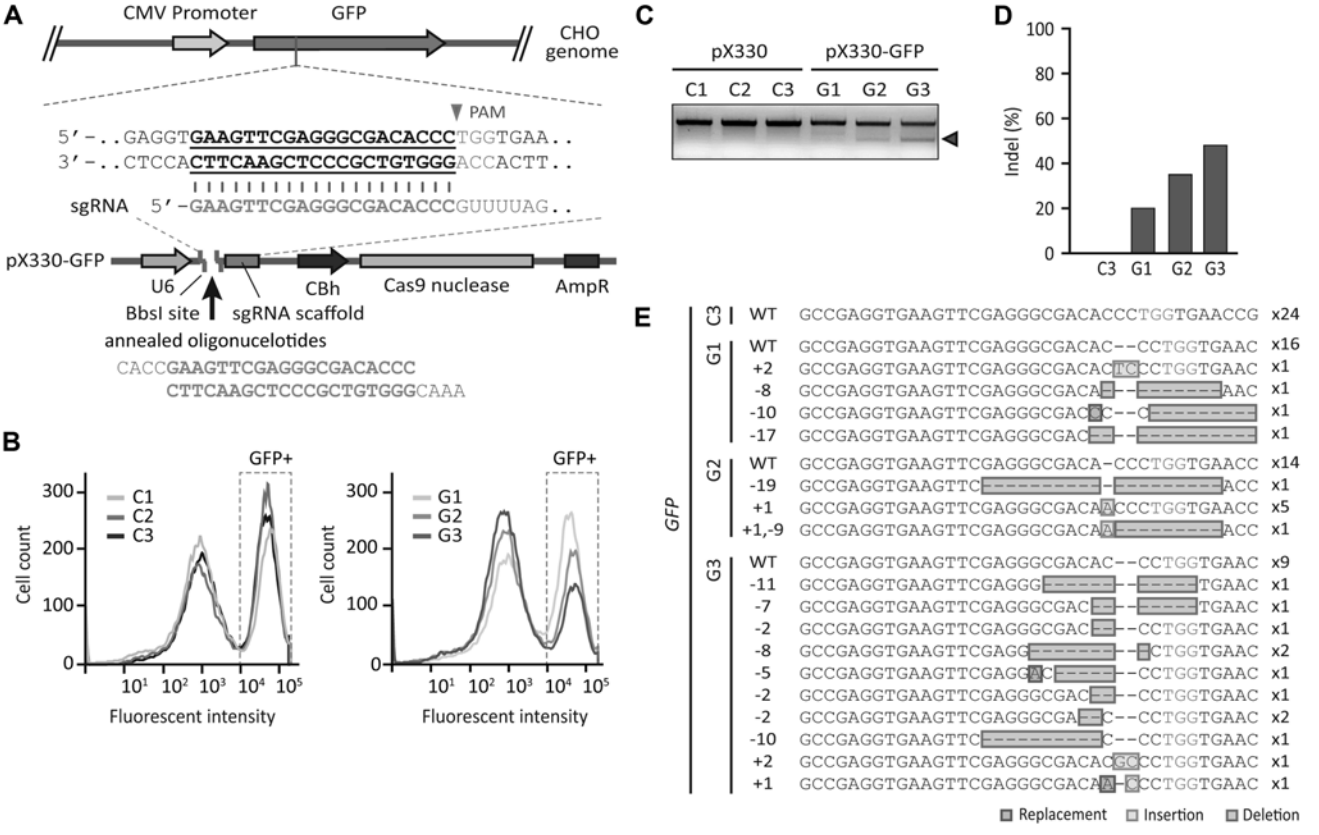

Fig. 1. RGN-based CHO genome editing by iterative transfection. (A) Schematics of the RNA-based CHO genome editing methodology. Annealed oligonucleotides containing a guide RNA sequence were inserted into the BbsI restriction site in the pX330 vector. The sgRNA transcribed from the pX330-GFP vector directs Cas9 nuclease to the *GFP* target site. (B) Quantitative analysis of GFP-positive cells measured by flow cytometry. The fractions of GFP-positive cells are shown by the green dotted line. Lanes are marked with either "C" or "G" to indicate control or GFP-expressing CHO cells, respectively. The number transfections carried out are indicated next to the respective letters. (C) T7E1 assay of *GFP*-specific RGN-mediated mutations. Red triangles indicate the expected DNA band after cleavage by T7E1. (D) TA-cloning based Sanger sequencing analysis of the mutations in the *GFP* target site that were generated by repetitive transfection. (E) Repetitive transfection of RGN vector induced mutations in the GFP target site. The wild type sequence is shown at the top, and the PAM sequence is shown in red. Red-, green-, and blue-colored boxes indicate deletions, insertions, and substitutions, respectively.

partially repaired by the indel-forming NHEJ pathway, which generates frame-shift indel mutations [11,21]. Accordingly, we expected that the frequency of small deletions or insertions in a given coding sequence could be increased by repetitive transfection. To test whether the iterative transfection method increased the indel rate, as compared to that obtained with a conventional, single transfection approach, we introduced a 20-nucleotide (nt) guide sequence into the sgRNA (Table 1), which was designed to abolish GFP fluorescence in CHO-K1 cells stably expressing a chromosomally integrated GFP (Fig. 1A). A population of stable CHO-GFP cells was established using a pEGFP-C1 vector. The sgRNA was expressed under the RNA polymerase III U6 promoter in a pX330 vector (pX330-GFP), targeting a locus (+339 ~ +359 nt from ATG), followed by a 5′-TGG protospacer-adjacent motif (PAM) sequence within the GFP coding sequence [11]. To maintain high-level expression of Cas9 nuclease and sgRNA, we iteratively transfected the CHO cells by using a DNA-Lipofectamine® 2000 vehicle every 8 h by replacing the culture medium. RGN-induced indel frequencies were then measured using flow cytometry, a mismatch-sensitive T7 endonuclease I (T7E1) assay, and Sanger sequencing (48 h post transfection).

A flow cytometry analysis showed that the iterative transfection of pX330-GFP abolished GFP fluorescence in up to 75% of the cells after 48 h post transfection (Fig. 1B). As expected, the fraction of cells expressing GFP in the third round of transfection (25%) was significantly decreased as compared to that in the first (46%) and second rounds of transfection (34%). By contrast, control experiments (CHO-GFP cells iteratively transfected with pX330 in the absence of sgRNA) showed no significant change in GFP fluorescence when subjected to iterative transfections. A T7E1 assay using the PCR-amplified DNA fragments of the edited genomic locus produced no detectable NHEJ-associated mutations in the control experiments, whereas GFP-specific RGN-induced mutations were detected in CHO-GFP cells iteratively transfected with pX330-GFP (Fig. 1C). The T7E1 band intensity increased with repetitive pX330-GFP treatment, indicating the accumulation of NHEJ-associated mutations in the targeted GFP locus. As an additional confirmation of RGN-mediated mutations, we performed TA cloning of the edited locus, followed by Sanger sequencing. Since the molecular signatures of the error-prone NHEJ-associated mutation result in small deletions, insertions, or replacements [22], we calculated the indel levels from our sequencing results. The indel level from the third round of pX330-GFP transfection was 48%, whereas the first round of transfection produced an indel level of only 20% (Figs. 1D and 1E).

Next, to investigate whether iterative transfection increased indel levels in endogenous genes, two sgRNAs were designed for the 5′ constitutive exons of *Efemp1* and *Fos* genes (Fig. 2A), encoding for the EGF containing fibulin-

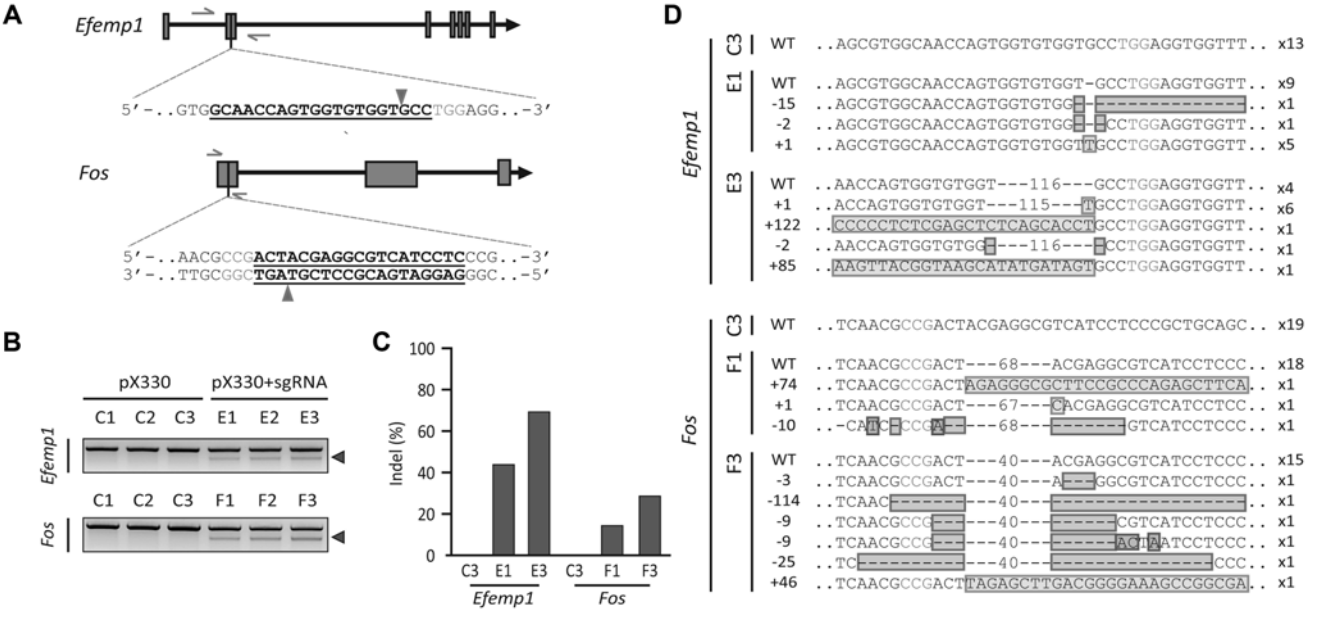

Fig. 2. RGN-based endogenous gene editing. (A) Target regions for editing *Efemp1* and *Fos* genes. The PAM sequence is shown in red, and the sgRNA site is shown in a bold font and is underlined. The red triangles indicate the target site for RGN. The pair of red arrows indicates the position of primers used for nested and hemi-nested PCR. (B) T7E1 assay of indel frequencies at *Efemp1* and *Fos* sites. Red triangles indicate the expected DNA band after cleavage by T7E1. (C) TA-cloning based Sanger sequencing analysis at *Efemp1* and *Fos* sites. (D) Analysis of indels in *Efemp1* and *Fos* sites. The wild type sequence is shown at the top. The PAM sequence and mismatched bases are shown in red. Red-, green-, and blue-colored boxes indicate deletions, insertions, and substitutions, respectively.

like extracellular matrix protein and the c-fos proto-oncogene, respectively [23,24]. T7E1 assays targeting *Efemp1* and *Fos* genes showed accumulating molecular signatures of error-prone NHEJ-associated mutations upon iterative transfection (Fig. 2B). Sanger sequencing of the PCR amplicon from targeted loci in CHO cells treated by the third round of transfection reached indel levels of 69 and 29% for *Efemp1* and *Fos* genes, respectively. By contrast, the first round of transfection produced indel levels of 44 and 14% for *Efemp1* and *Fos* genes, respectively (Fig. 2C, D).

Consequently, indel levels targeting the endogenous genes were increased by approximately 150 ~ 200% by using the iterative transfection approach, consistent with our observation of enhanced editing efficiency in the chromosomally integrated GFP gene. Although efficiency of the genome editing varied significantly among the target regions, the enhancement ratio of editing efficiency was almost the same. Regardless of editing efficiency, iterative transfection can be more robust method for the RGN-mediated genome editing than the traditional method.

3.2. Multiplex genome editing by using iterative transfection

Considering the enhanced efficiency yielded by iterative RNG-mediated mutagenesis, we sought to determine the feasibility of multiplex genome editing for the simultaneous disruption of multiple targets. To this end, we constructed pX330d_E_T (Fig. 3A), which expresses two sgRNA for targeting the 5′ constitutive exons of *Efemp1* and *Thbs1* genes (Figs. 2A and 3B). As expected, T7E1 assays showed increased indel levels for both targeted sites after three rounds of iterative transfection (Fig. 3C). In addition, sequencing of the PCR amplicons from the iterative transfection showed that 80 and 60% of the target sequences in the *Efemp1* and *Thbs1* genes, respectively, were mutated, whereas single transfection stimulated indel levels of 70 and 30%, respectively (Figs. 3D and 3E). Taken together, we conclude that the high-level expression of Cas9 nuclease and sgRNA achieved through an iterative transfection protocol induces a higher level of site-specific mutation, and the approach can be extended to multiple targets simultaneously, thereby permitting multiplex genome editing.

3.3. Relationship between the mutation frequencies and the level of sgRNA-Cas9 complex

To evaluate whether iterative transfection increased the expression levels of sgRNA and Cas9 nuclease, we

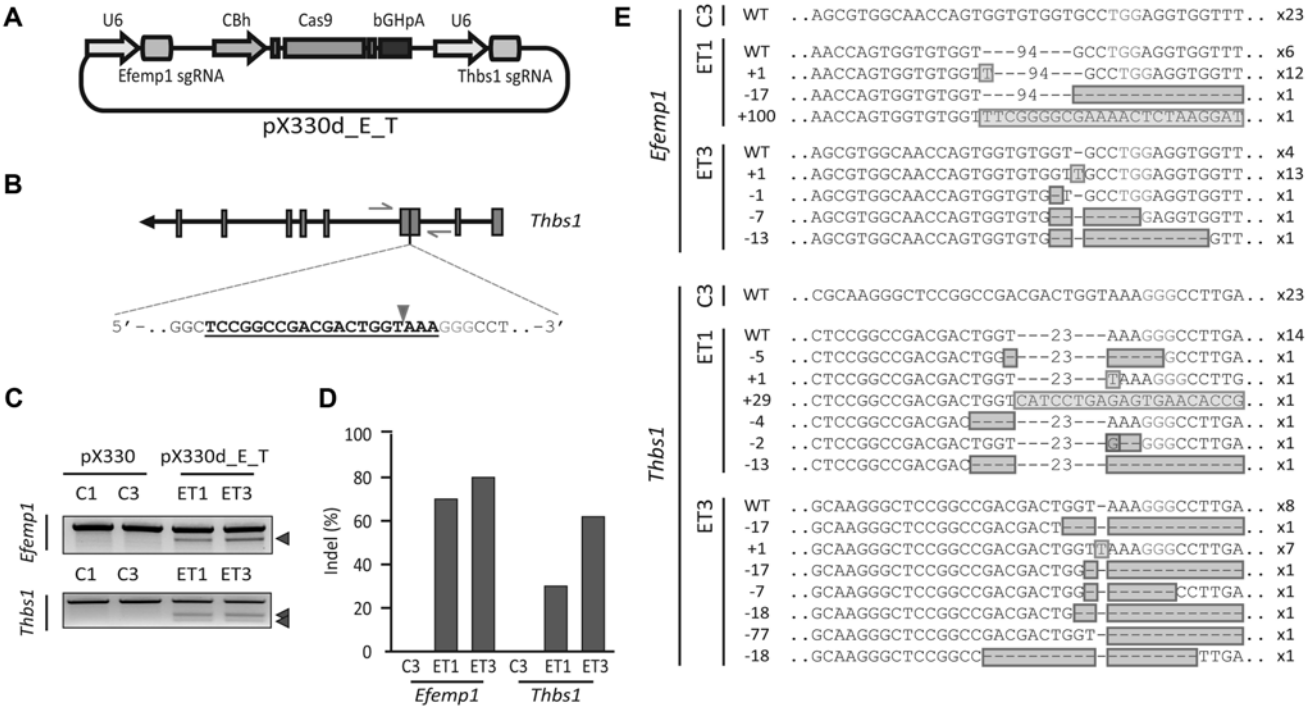

Fig. 3. Multiplex genome editing by using iterative transfection. (A) The map of pX330d_E_T. (B) Target regions for editing *Thbs1* genes. The PAM sequence is shown in red, and the sgRNA site is shown in a bold font and is underlined. The red triangles indicate the target site of RGN. The pair of red arrows indicates the position of primers used for nested and hemi-nested PCR. (C) T7E1 assay of indel frequencies at Efemp1 and Thbs1 sites. Red triangles indicate the expected DNA band after cleavage by T7E1. (D) TA-cloning based Sanger sequencing analysis at *Efemp1* and *Thbs1* sites. (E) Analysis of indels in *Efemp1* and *Thbs1* sites. The wild type sequence is shown at the top. The PAM sequence and mismatched bases are shown in red. Red-, green-, and blue-colored boxes indicate deletions, insertions, and substitutions, respectively.

performed qRT-PCR and western blot assays, respectively. The qRT-PCR results showed that sgRNA were rapidly degraded in cells (Fig. 4A). Although similar expression levels were observed 24 h post-transfection, the level of sgRNA 48 h post-transfection persisted in cells that had undergone multiple rounds of transfection, with each round of transfection producing greater expression levels. These results indicate that iterative transfection permits three-fold higher expression levels of sgRNA over the single transfection approach, lasting up to 48 h post-transfection.

Western blot analysis of Cas9 nuclease was similarly used to track protein levels in CHO cells subjected to iterative rounds of transfection. Similar levels of Cas9 were found 8 h post-transfection for single and iteratively transfected cells (Fig. 4B). However, cells that had undergone three rounds of transfection showed high Cas9 nuclease expression, persisting up to 72 h post-transfection, whereas the expression levels declined after 48 h post-transfection in cells that had undergone only a single round of transfection. Notably for single transfections, the levels of Cas9 nuclease and sgRNA peaked at different times, presumably resulting in suboptimal levels of the sgRNA-Cas9 nuclease complex. By comparison, the repetitive transfection approach maintained balanced levels of both sgRNA and Cas9 nuclease for optimal levels of sgRNA-Cas9 complex, likely accounting for the observed enhancement in editing efficiency.

We then investigated whether mutation frequencies are dependent on the level of sgRNA-Cas9 complex formation. It is difficult to control precisely the expression of Cas9 nuclease and sgRNA *in vivo*, whereas the molar ratio of purified Cas9 and *in vitro* transcribed sgRNA can be controlled easily *in vitro* before transfection. For sgRNA-Cas9 nuclease complex delivery *in vitro*, *E.coli* BL21 (DE3) strain was transformed with the plasmid pET28a/Cas9-Cys containing Cas9 nuclease translationally fused to an N-terminal 6x His-tag [17]. Cas9 nuclease was purified using Ni-NTA agarose beads, mixed with *in vitro* transcribed sgRNA and transfected with the resulting sgRNA-Cas9 nuclease complex into CHO cells using Lipofectamine [25]. T7E1 assay showed that increasing molar concentration of sgRNA up to 150 nM resulted in an increase in gene mutation frequencies (Fig. 4C). Collectively these results suggest that the high-level of sgRNA-Cas9 complex required to maximize mutation frequencies.

3.4. Effect of iterative transfection on off-target editing

Recent studies have reported that off-target effects are induced by RGN. The sequences of on-target and off-target sites differed by five nucleotides in other mammalian cells [14,26]. To evaluate the off-target effects induced by our iterative transfection approach, potential off-target sites

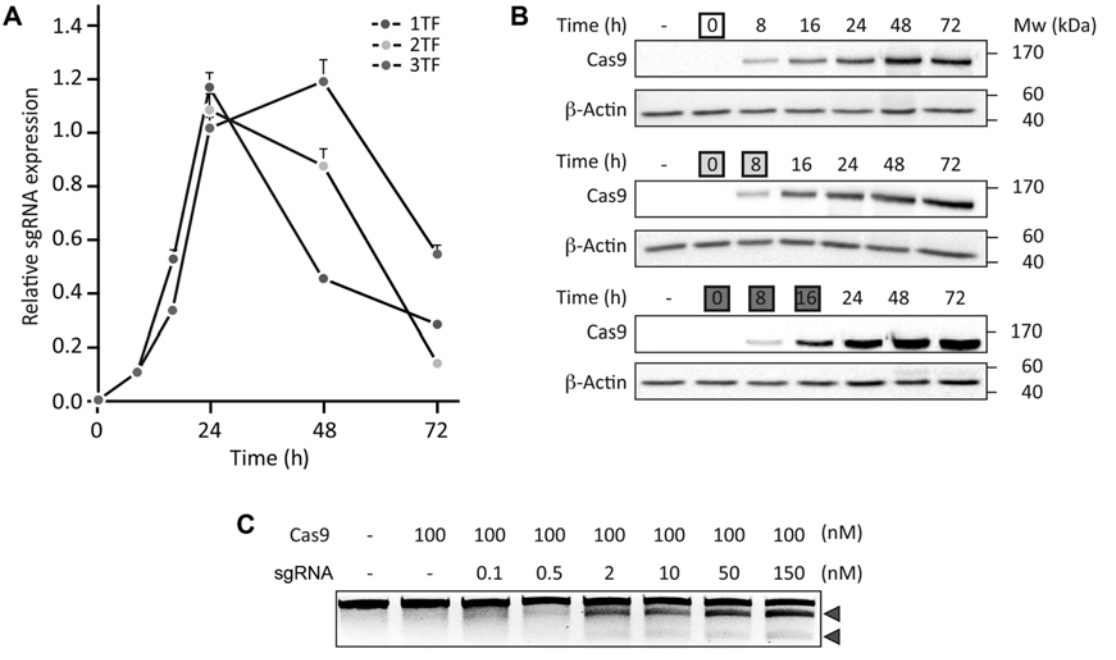

Fig. 4. Balanced expression of sgRNA and Cas9 nuclease. (A) Time-course analyses of the expression of sgRNA and Cas9 nuclease. qRT-PCR of the repetitively transfected CHO-GFP cells showing the abundance relative to sgRNA. mRNA transcripts of sgRNA were compared to those of actin (control). Data are represented as mean ± SEM from technical replicates (n = 3). (B) Western blot analysis of repetitively transfected CHO-GFP cells showing the relative abundance of Cas9 nuclease. Blotting with anti-β-actin antibody was used as an experimental control. White, yellow, and red boxes represent the number of transfections. (C) T7E1 assay of indel frequencies at *Fos* site. Red triangles indicate the expected DNA band after cleavage by T7E1.

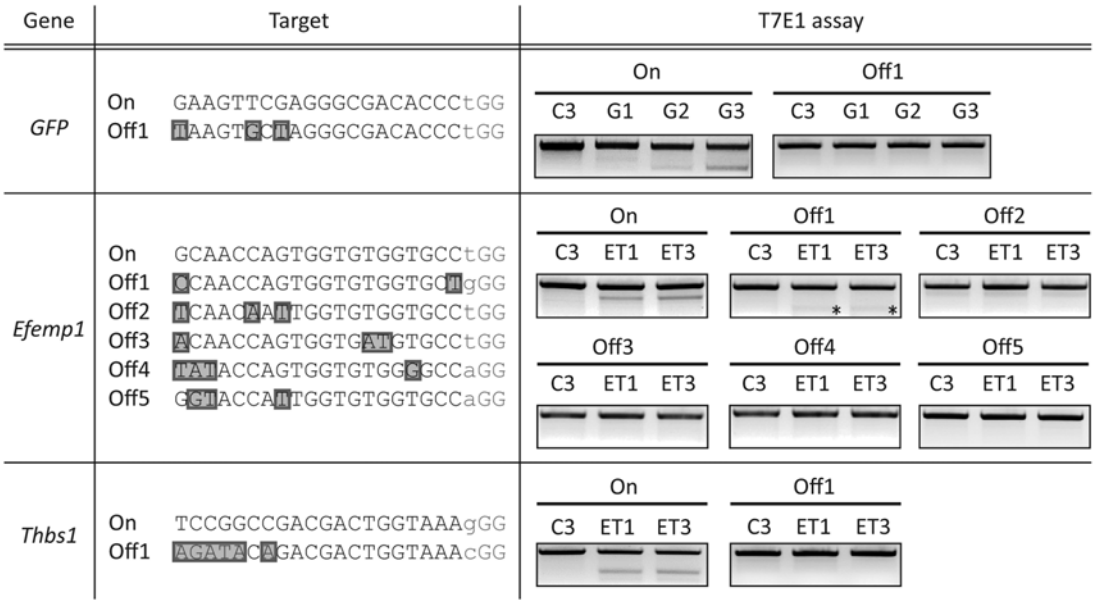

Fig. 5. Analysis of off-target effects. Mutation frequencies at potential off-target sites were detected using the T7E1 assay. The PAM sequence and mismatched bases are shown in red and blue, respectively. Asterisks mark the expected DNA band positions upon T7E1 cleavage.

having sequences that were similar to those of our target genes (*GFP*, *Efemp1*, or *Thbs1*) were investigated in the CHO cells (Fig. 3). Briefly, 22-nt off-target sites containing PAM sequences that differed from the on-target sites by six nucleotides or less were identified. Based on the results from our T7E1 assays, no nucleotides were altered by three or more bases at six of the evaluated off-target sites (GFP-OFF1, Efemp1-Off2 to Efemp1-Off5, and Thbs1-Off1). An error-prone NHEJ-associated mutation was detected at one off-target site in the *Efemp1* gene (Efemp1-Off1) that contained a two-base mismatch. These results suggest that repetitive transfection does not increase the indel rate at putative off-target sites.

4. Conclusion

The programmable RGN system has emerged as an efficient and robust genome editing strategy, allowing for the deletion, addition, or replacement of sequences at points of interest in cells ranging from bacterial to human origin [9,16]. However, one of the critical determinants for increasing the indel rate and ultimately the success of the approach is the synchronous enhancement of both guide RNA and Cas9 nuclease expression in the nucleus. Single transfections of the RGN vector showed relatively lower expression of sgRNA and Cas9 nuclease as compared with that observed using iterative transfections; additionally, single transfections resulted in imbalanced expression levels of sgRNA and Cas9 nuclease. In contrast, by using iterative transfections, we achieved approximately three-fold higher expression levels for Cas9 nuclease and sgRNA over that obtained using the conventional single transfection method. As a result of the increased abundance of sgRNA and Cas9 nuclease, sgRNA and Cas9 nuclease expression levels seemed to peak at similar time points in principle, allowing for a greater degree of complex formation, thereby generating relatively higher rates of mutation. To confirm these results, we controlled the amount of sgRNA-Cas9 complex formation *in vitro* and delivered the complex directly. As a result, the high-level of sgRNA-Cas9 complex enables efficient genome editing. Additionally, we have demonstrated multiplex genome editing for two target genes without increasing mutation rates of putative off-target sites. Conceivably, the multiplex genome engineering could be extended to an even greater number of targets [27-29]. In conclusion, we have demonstrated that the application of iterative transfections to the CRISPR/Cas9 technology enables a relatively simple and efficient means of enhancing target-specific genome editing, a tool that allows for single or multiple site-directed mutagenesis to be carried out in an increasingly useful CHO cell line.

Acknowledgement

This research was supported by the Intelligent Synthetic Biology Center for Global Frontier Project (2011-0031962)

and the Bio & Medical Technology Development Program of the National Research Foundation (NRF), funded by the Ministry of Science, ICT & Future Planning (NRF-2013M3A9B6075931).

References

1. Datta, P., R. J. Linhardt, S. T. and Sharfstein (2013) An 'omics approach towards CHO cell engineering. *Biotechnol. Bioeng.* 110: 1255-1271.
2. Steentoft, C., Vakhrushev, S. Y., Vester-Christensen, M. B., Schjoldager, K. T., Kong, Y., Bennett, E. P., U. Mandel, H. Wandall, S. B. Levery, and H.Clausen (2011) Mining the O-glycoproteome using zinc-finger nuclease-glycoengineered SimpleCell lines. *Nat. Methods*. 8: 977-982.
3. Meuris, L., F. Santens, G. Elson, N. Festjens, M. Boone, A. Dos Santos, S. Devos, F. Rousseau, E. Plets, E. Houthuys, P. Malinge, G. Magistrelli, L. Cons, L.Chatel, B. Devreese, and N. Callewaert (2014) GlycoDelete engineering of mammalian cells simplifies N-glycosylation of recombinant proteins. *Nat. Biotechnol*. 32: 485-489.
4. Ronda, C., L. E. Pedersen, H. G. Hansen, T. B. Kallehauge, M. J. Betenbaugh, A. T. Nielsen, and H. F. Kildegaard (2014) Accelerating genome editing in CHO cells using CRISPR Cas9 and CRISPy, a web-based target finding tool. *Biotechnol. Bioeng.* 111: 1604-1616.
5. Xu, X., H. Nagarajan, N. E. Lewis, S. Pan, Z. Cai, X. Liu, W. Chen, M. Xie, W. Wang, S. Hammond, M. R. Andersen, N. Neff, B. Passarelli, W. Koh, H. C. Fan, J. Wang, Y. Gui, K. H. Lee, M. J. Betenbaugh, S. R. Quake, I. Famili, B. O. Palsson, and J. Wang (2011) The genomic sequence of the Chinese hamster ovary (CHO)-K1 cell line. *Nat. Biotechnol*. 29: 735-741.
6. Lewis, N. E., X. Liu, Y. Li, H. Nagarajan, G. Yerganian, E. O'Brien, A. Bordbar, A. M. Roth, J. Rosenbloom, C. Bian, M. Xie, W. Chen, N. Li, D. Baycin-Hizal, H. Latif, J. Forster, M. J. Betenbaugh, I. Famili, X. Xu, J. Wang, and B. O. Palsson (2013) Genomic landscapes of Chinese hamster ovary cell lines as revealed by the Cricetulus griseus draft genome. *Nat. Biotechnol*. 31: 759-765.
7. Sealover, N. R., A. M. Davis, J. K. Brooks, H. J. George, K. J. Kayser, and N. Lin (2013) Engineering Chinese hamster ovary (CHO) cells for producing recombinant proteins with simple glycoforms by zinc-finger nuclease (ZFN)-mediated gene knockout of mannosyl (alpha-1,3-)-glycoprotein beta-1,2-N-acetylglucosaminyltransferase (Mgat1). *J. Biotechnol.* 167: 24-32.
8. Carlson, D. F., S. C. Fahrenkrug, and P. B. Hackett (2012) Targeting DNA With Fingers and TALENs. *Mol. Ther. Nucleic acids*. 1: e3.
9. Sander, J. D. and J. K. Joung (2014) CRISPR-Cas systems for editing, regulating and targeting genomes. *Nat. Biotechnol*. 32: 347-355.
10. Mali, P., L. Yang, K. M. Esvelt, J. Aach, M. Guell, J. E. DiCarlo, J. E. Norville, and G. M. Church (2013) RNA-guided human genome engineering *via* Cas9. *Science*. 339: 823-826.
11. Cong, L., F. A. Ran, D. Cox, S. Lin, R. Barretto, N. Habib, P. D. Hsu, X. Wu, W. Jiang, L. A. Marraffini, and F. Zhang (2013) Multiplex genome engineering using CRISPR/Cas systems. *Sci*. 339: 819-823.
12. Deveau, H., J. E. Garneau, and S. Moineau (2010) CRISPR/Cas system and its role in phage-bacteria interactions. *Ann. Rev. Microbiol*. 64: 475-493.
13. Cho, S. W., S. Kim, J. M. Kim, and J. S. Kim (2013) Targeted genome engineering in human cells with the Cas9 RNA-guided endonuclease. *Nat. Biotechnol*. 31: 230-232.
14. Fu, Y., J. A. Foden, C. Khayter, M. L. Maeder, D. Reyon, J. K. Joung, and J. D. Sander (2013) High-frequency off-target mutagenesis induced by CRISPR-Cas nucleases in human cells. *Nat. Biotechnol*. 31: 822-826.
15. Jiang, W., D. Bikard, D. Cox, F. Zhang, and L. A. Marraffini (2013) RNA-guided editing of bacterial genomes using CRISPR-Cas systems. *Nat. Biotechnol*. 31: 233-239.
16. Hsu, P. D., E. S. Lander, and F. Zhang (2014) Development and applications of CRISPR-Cas9 for genome engineering. *Cell*. 157: 1262-1278.
17. Ramakrishna, S., A. B. Kwaku Dad, J. Beloor, R. Gopalappa, S. K. Lee, and H. Kim (2014) Gene disruption by cell-penetrating peptide-mediated delivery of Cas9 protein and guide RNA. *Genome Res.* 24: 1020-1027.
18. Duda, K., L. A. Lonowski, M. Kofoed-Nielsen, A. Ibarra, C. M. Delay, Q. Kang, Z. Yang, S. M. Pruett-Miller, E. P. Bennett, H. H. Wandall, G. D. Davis, S. H. Hansen, and M. Frodin (2014) High-efficiency genome editing *via* 2A-coupled co-expression of fluorescent proteins and zinc finger nucleases or CRISPR/Cas9 nickase pairs. *Nucleic Acids Res*. 42: e84.
19. Kim, N. S., T. H. Byun, and G. M. Lee (2001) Key determinants in the occurrence of clonal variation in humanized antibody expression of cho cells during dihydrofolate reductase mediated gene amplification. *Biotechnol. Progr.* 17: 69-75.
20. Ghorbaniaghdam, A., J. Chen, O. Henry, and M. Jolicoeur (2014) Analyzing clonal variation of monoclonal antibody-producing CHO cell lines using an *in silico* metabolomic platform. *PloS One*. 9: e90832.
21. Shalem, O., N. E. Sanjana, E. Hartenian, X. Shi, D. A. Scott, T. S. Mikkelsen, D. Heckl, B. L. Ebert, D. E. Root, J. G. Doench, and F. Zhang (2014) Genome-scale CRISPR-Cas9 knockout screening in human cells. *Sci*. 343: 84-87.
22. Santiago, Y., E. Chan, P. Q. Liu, S. Orlando, L. Zhang, F. D. Urnov, M. C. Holmes, D. Guschin, A. Waite, J. C. Miller, E. J. Rebar, P. D. Gregory, A. Klug, and T. N. Collingwood (2008) Targeted gene knockout in mammalian cells by using engineered zinc-finger nucleases. *Proc. Natl. Acad. Sci. USA* 105: 5809-5814.
23. McLaughlin, P. J., B. Bakall, J. Choi, Z. Liu, T. Sasaki, E. C. Davis, A. D. Marmorstein, and L. Y. Marmorstein (2007) Lack of fibulin-3 causes early aging and herniation, but not macular degeneration in mice. *Hum. Mol. Genet*. 16: 3059-3070.
24. Ranjan, V., R. Waterbury, Z. Xiao, and S. L. Diamond (1996) Fluid shear stress induction of the transcriptional activator c-fos in human and bovine endothelial cells, HeLa, and Chinese hamster ovary cells. *Biotechnol. Bioeng*. 49: 383-390.
25. Zuris, J. A., D. B. Thompson, Y. Shu, J. P. Guilinger, J. L. Bessen, J. H. Hu, M. L. Maeder, J. K. Joung, Z. Y. Chen, and D. R. Liu (2015) Cationic lipid-mediated delivery of proteins enables efficient protein-based genome editing *in vitro* and *in vivo*. *Nat. Biotechnol*. 33: 73-80.
26. Pattanayak, V., S. Lin, J. P. Guilinger, E. Ma, J. A. Doudna, and D. R. Liu (2013) High-throughput profiling of off-target DNA cleavage reveals RNA-programmed Cas9 nuclease specificity. *Nat. Biotechnol*. 31: 839-843.
27. Sakuma, T., A. Nishikawa, S. Kume, K. Chayama, and T. Yamamoto (2014) Multiplex genome engineering in human cells using all-in-one CRISPR/Cas9 vector system. *Sci. Rep*. 4: 5400.
28. Hsu, P. D., D. A. Scott, J. A. Weinstein, F. A. Ran, S. Konermann, V. Agarwala, Y. Li, E. J. Fine, X. Wu, O. Shalem, T. J. Cradick, L. A. Marraffini, G. Bao, and F. Zhang (2013) DNA targeting specificity of RNA-guided Cas9 nucleases. *Nat. Biotechnol*. 31: 827-832.
29. Kim, S., D. Kim, S. W. Cho, J. Kim, and J. S. Kim (2014) Highly efficient RNA-guided genome editing in human cells *via* delivery of purified Cas9 ribonucleoproteins. *Genome Res*. 24: 1012-1019.